A Dynamic Ocean–Atmosphere Model of the Tropical Atlantic Decadal Variability

SHANG-PING XIE

Graduate School of Environmental Earth Science, Hokkaido University, Sapporo, Japan

(Manuscript received 29 August 1997, in final form 13 January 1998)

ABSTRACT

A linear model that couples an ocean mixed layer with a simple dynamic atmosphere is used to study the mechanism for decadal variability over the tropical Atlantic. An unstable mode with a dipole sea surface temperature (SST) pattern similar to observed decadal variability in the tropical Atlantic emerges in the time integration of the model. A wind–evaporation–SST feedback is responsible for the growth and oscillation of the unstable mode whereas the mean state of the Atlantic climate is essential for maintaining the spatially quasi-standing dipole structure. The oscillation period ranges from several to a few tens of years and is sensitive to coupling strength.

The oscillation is not self-sustainable as the realistic damping rate exceeds the growth rate. In response to white noise forcing, the model produces a red SST spectrum without a peak at finite frequencies. Therefore it is suggested that the tropical dipole's preferred timescales, if any, arise from the forcing by or interaction with the extratropics. In a model run where the forcing is confined to the extratropics, a dipole SST pattern still dominates the forcing-free Tropics, in support of the proposed linkage between the Tropics and extratropics.

1. Introduction

The sea surface temperature (SST) field over the tropical Atlantic Ocean displays significant variability on both interannual and decadal time scales. The Atlantic interannual variability is analogous to El Niño–Southern Oscillation in the Pacific, involving the interaction of zonal winds, thermocline depth and SST in the equatorial strip (Zebiak 1993; Carton et al. 1996). The decadal SST variability, on the other hand, is most pronounced off the equator around 10–15°N/S, with the northern anomaly taking the opposite polarity of the southern one (Moura and Shukla 1981, among others). This dipole mode of SST variability affects the seasonal excursion of the intertropical convergence zone (ITCZ), causing rainfall variability over Northeast Brazil (Hastenrath and Heller 1977) and the Sahel (Lamb 1978).

Recent modeling studies indicate that wind-induced changes in surface latent heat flux are the main cause of the decadal SST dipole. In an ocean general circulation model (GCM), the decadal SST dipole disappears when the wind speed variability is removed from surface heat flux calculation. In contrast its phase and amplitude are well reproduced in a run where the wind variability is removed from momentum but retained in heat flux calculation (Carton et al. 1996). An analysis of the mixed layer heat budget based on observational data confirms that wind-induced fluctuations in surface latent heat flux is the major cause of the SST dipole (Wagner 1996). Based on a singular value decomposition analysis, Chang et al. (1997) derive an empirical relation between the spatial structures of SST and surface heat flux anomalies. Coupling this empirical atmosphere model with ocean models, Chang et al. find that the interaction of heat flux and SST gives rise to decadal oscillations similar to the observed Atlantic dipole.

A positive ocean–atmosphere feedback involving wind, evaporation, and SST (WES) seems at work in sustaining the coupled decadal oscillation. Figure 1 displays four oscillation indices as a function of time [see Nobre and Shukla (1996) and Chang et al. (1997) for spatial structures]. SST and surface wind oscillate in phase with each other. This oscillation was weak in the 1950s and 60s but became pronounced from late 1960s. During high-index periods with positive (negative) SST anomalies to the north (south) of the equator, a northward pressure gradient is set up, driving southerly cross-equatorial winds. Deflected by Coriolis force, these southerly winds induce westerly (easterly) wind anomalies and thus weaken (intensify) the prevailing background easterly winds north (south) of the equator. Such changes in wind speed reduce (enhance) surface evaporation north (south) of the equator, amplifying the initial north–south SST difference. This WES feedback is originally proposed by Xie and Philander (1994) to explain the equatorial asymmetry of the Pacific climatol-

Corresponding author address: Dr. Shang-Ping Xie, Graduate School of Environmental Earth Science, Hokkaido University, Sapporo 060-0810, Japan.
E-mail: xie@ees.hokudai.ac.jp

© 1999 American Meteorological Society

Unauthenticated | Downloaded 05/27/24 07:30 AM UTC

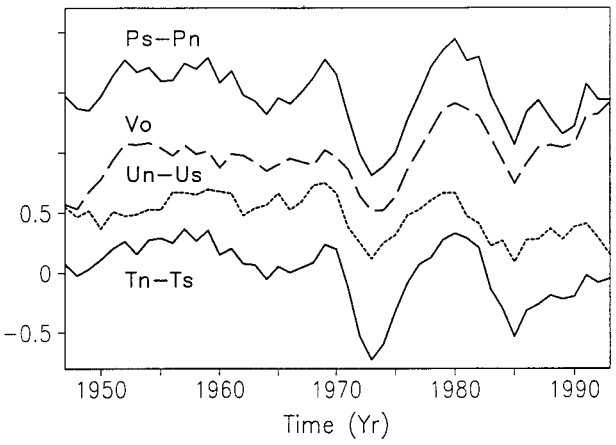

FIG. 1. Indices of the tropical Atlantic decadal oscillation as a function of time: meridional wind speed (V in m s^{-1}) averaged between 5°S and 5°N, north–south differences in sea level pressure (P in mb), zonal wind speed (U in m s^{-1}), and sea surface temperature (T in °C) between zonal averages within 5°N–25°N and 5°S–25°S. Three-point running mean is applied to annual-mean anomalies based on the Comprehensive Ocean–Atmosphere Dataset (Woodruff et al. 1987). The curves for U, V, and P are offset by 0.5 units successively.

ogy, most notably the Northern Hemisphere ITCZ. For this reason, previous studies tend to focus on nonoscillatory WES modes (see Xie 1996 for a review). The only oscillatory solution reported so far looks very different from the observed Atlantic dipole, showing rapid equatorward phase propagation (Xie 1997). While observations and ocean GCM experiments consistently implicate the WES feedback, dynamic coupled models fail to demonstrate so.

In an attempt to resolve this paradox, this study reexamines the WES instability and investigates processes affecting its frequency and meridional structure. A modified version of Xie's (1997) model is used, which couples a mixed layer ocean with a simple dynamic model of the atmosphere. We will show that the mean state around which the model is linearized has a large impact on the spatial structures of the dominant WES mode. By including a mean state typical of the Atlantic, the model is capable of simulating a decadal dipole mode whose spatial structures resemble observations. Compared with previous models that successfully simulate the dipole oscillation (Mehta and Delworth 1995; Chang et al. 1997), the present one is very simple, allowing insight into responsible physics. One major difference between Chang et al.'s and the present models lies in the treatment of the atmosphere. They employ an empirical atmosphere model that predetermines the spatial structures of the coupled mode, whereas we use a dynamic model where both the temporal and spatial structures are determined by internal coupled dynamics.

The rest of the paper is organized as follows: the next section describes the model while section 3 examines its free mode. Section 4 analyzes the model response to external forcing. Section 5 summarizes the paper and offers a mechanism to link the decadal modes from the south to the north over the whole Atlantic Ocean.

TABLE 1. Model parameters.

A^{-1}	2 day	c_p	4×10^3 J kg^{-1}K^{-1}
C	45 m s^{-1}	h	50 m
K	3.5×10^{-1} m s^{-1}K^{-1}	κ	2×10^3 m^{2}s^{-1}
C_E^*	1×10^3 J m^{-3}	C_D^*	1×10^{-2} Ns m^{-3}
L	2.5×10^6 J kg^{-1}	ε_s^{-1}	2 day
R^*	462 J kg^{-1}K^{-1}	b^{-1}	1 yr
ρ	1×10^3 kg m^{-3}		

2. Model

To the first order, the tropical Atlantic dipole pattern may be viewed as zonally uniform. Hence we only consider zonally symmetric cases and focus on the north–south interaction.

a. The atmosphere

The Matsuno (1966)–Gill (1980) model is used for the atmosphere:

$$\varepsilon U - YV = 0, \tag{2.1}$$

$$\varepsilon V + YU = -\Phi_Y, \tag{2.2}$$

$$\varepsilon \Phi + V_Y = -KT, \tag{2.3}$$

where U and V are the zonal and meridional components of surface wind velocity, $\Phi = \varphi/C$ with φ being the geopotential and C the long gravity wave speed, $Y = y(\beta/C)^{1/2}$ is the nondimensional meridional coordinate with β the latitudinal gradient of the Coriolis parameter, $\varepsilon = A/(\beta C)^{1/2}$ is the nondimensional damping rate with A being its dimensional counterpart, T is the SST perturbation and K the coupling coefficient. Model parameters and their typical value are listed in Table 1.

Significant precipitation anomalies associated with the tropical dipole are limited to small equatorial regions and to boreal spring (Nobre and Shukla 1996). Over most of the Tropics SST anomalies seem to affect surface winds via changes in boundary layer temperature (Linzden and Nigam 1987; Neelin 1989). A positive (negative) SST anomaly warms (cools) air aloft in the boundary layer, thus inducing a low (high) pressure at the sea surface.

b. The ocean

The ocean model is intended to be as simple as possible yet contain physics essential for the decadal SST dipole. In light of results from an ocean GCM simulation of the Atlantic dipole (Carton et al. 1996), the latent heat flux at the ocean surface will be treated not just as a thermal damping but a function of wind speed as well. We will neglect the upwelling effect, which is presumably small because of the prevailing Ekman downwell-

Unauthenticated | Downloaded 05/27/24 07:30 AM UTC

ing off the equator. This filters out the equatorial mode (Zebiak 1993) where upwelling is a dominant mechanism for SST change. Since the decadal variations in SST and wind are small relative to their mean values, we may linearize the ocean thermodynamic equation and obtain a linear equation for mixed layer temperature perturbation T

$$T_t + \overline{v}T_y + v\overline{T}_y = aU - bT + \kappa T_{yy}, \quad (2.4)$$

where the overbar denotes the mean state variable, subscripts denote partial derivatives, and b is the coefficient for Newtonian damping arising from both temperature dependence of evaporation and background mixing. The time–space characteristics of the WES mode are sensitive to the diffusivity κ (Xie 1997), which is here chosen to be 2×10^3 m^2 s^{-1}, a value commonly used in ocean models.

The first term on the rhs of (2.4) is obtained by linearizing the evaporation term

$$E = C_E^*|\overline{U} + U|q(T)$$
$$= C_E^*\left[-\overline{U}\overline{q} - U\overline{q} + \frac{L}{R^*\overline{T}^2}\overline{U}\overline{q}T + o(T^2, UT, V^2)\right], \quad (2.5)$$

where $C_E^* = \rho_a L C_E(1 - \text{RH})$ is an evaporation coefficient with ρ_a, L and RH being air density, latent heat and relative humidity, respectively, and $q = q_0 \exp[(L/R^*)(1/T_0 - 1/T)]$ is the Clausius–Clapeyron equation for saturated specific humidity with R* being the water vapor gas constant. The basic-state wind speed $\overline{U}$ should be nonzero but can be either easterly or westerly, with the easterly wind case being relevant to the tropical Atlantic. Meridional wind perturbation appears as a higher order term in (2.5) because $|\overline{V}/\overline{U}| \ll 1$ near centers of the SST dipole. The coefficient for the WES feedback is thus

$$a = \left(\frac{1}{-\overline{U}}\right)\frac{\overline{E}}{c_p\rho h}, \quad (2.6)$$

where c_p and ρ are the specific heat at constant pressure and density of water, h is the mixed layer depth that will be set constant for simplicity. Further we will not consider effects of seasonal cycle and clouds.

An Ekman layer model (e.g., Zebiak and Cane 1987) is used to compute surface ocean currents. In particular, a zonal wind stress induces a meridional Ekman flow

$$v = -b_u U, \quad (2.7)$$

with $b_u = [f/(f^2 + \varepsilon_s^2)](C_D^*/\rho h)$ where ε_s is the mechanical damping rate and a linear drag law is used with C_D^* being the drag coefficient. We will not consider the advection by geostrophic current that is generally weak relative to Ekman flow in the interior ocean. An explicit calculation of geostrophic flow requires including more complex ocean dynamics and is left for future study. Substituting (2.7) in (2.4) yields

$$T_t + \overline{v}T_y = (a + b_u\overline{T}_y)U - bT + \kappa T_{yy}. \quad (2.8)$$

Since $\overline{T}_y \le 0$ outside a small equatorial strip, the advection by perturbation Ekman flow weakens (enhances) the WES feedback in the Tropics (midlatitudes) where easterly (westerly) winds prevail.

A basic state typical of the tropical Atlantic is prescribed, with mean easterly winds,

$$\overline{U} = -3[1 + \sin(\pi y/2000 \text{ km})] \quad \text{m s}^{-1}, \quad (2.9)$$

driving a poleward mean Ekman flow according to (2.7). The mean SST is uniformly 30°C within 15° of the equator and then decreases with latitude

$$T/T_0 = \begin{cases} 1, & |y| < 1500 \text{ km} \\ 1 - G|y|, & |y| > 1500 \text{ km}, \end{cases} \quad (2.10)$$

with $G = 1$ K (200 km)$^{-1}$. This SST distribution causes the WES feedback coefficient (a) to decrease poleward. The sign of a depends on the mean wind direction, being positive (negative) for mean easterly (westerly) wind. Near the boundary between the mean easterly and westerly wind regimes at 30°, a should vanish. In the model, a is modified poleward of $y = 2500$ km and is gradually brought to zero at $y = 3000$ km. This modification of a turns out to have only a minor effect on model results. The above basic state is symmetric about the equator, an idealization of the Atlantic where the northern ITCZ appears to be the axis of symmetry for the dipole.

c. Unstable condition

An unstable condition for a disturbance to grow can be derived by forming a SST variance equation. Multiplying (2.8) by T and integrating it over the model domain gives rise to

$$\langle T^2\rangle_t/2 = \langle(a + b_u\overline{T}_y)UT\rangle + \langle\overline{v}_y T^2\rangle/2 - b\langle T^2\rangle - \kappa\langle(T_y)^2\rangle, \quad (2.11)$$

where $\langle\ \rangle$ denotes the area integral. Because the mean Ekman pumping is downward ($\overline{v}_y < 0$) outside a small equatorial region where T is small, the second term on the rhs is negative. Thus, the WES feedback, the first term on the rhs, is the only destabilizing mechanism in the model. Positive covariance between zonal wind and SST anomalies is the condition for the temporal growth of a coupled disturbance.

In the present model SST anomalies are caused by wind-induced evaporation and modified by Ekman advection. A simpler case with a uniform basic state and zero Ekman advection is studied by Xie (1997). Here the model is solved numerically by time stepping and space difference with a resolution of 50 km. The model domains extends from 30°S to 30°N for the ocean and 45°S to 45°N for the atmosphere. Vanishing lateral heat flux condition is applied to the poleward boundaries of the ocean. The model is integrated for several cycles of oscillation until a stable modal structure is obtained.

Unauthenticated | Downloaded 05/27/24 07:30 AM UTC

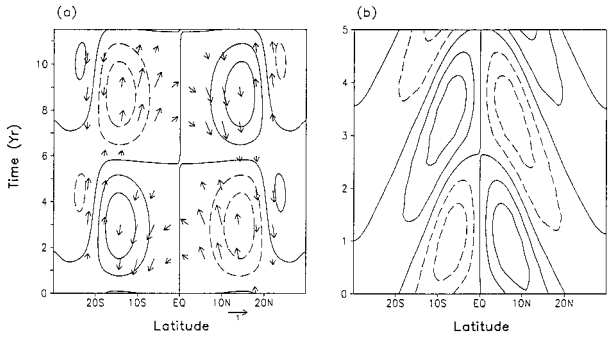

FIG. 2. Latitude–time section of sea surface temperature (contours with the negative ones dashed) and surface wind velocity (vectors) associated with the free WES mode in models (a) with and (b) without the mean Ekman advection. The exponential growth trend is removed. Easterly wind appears as an upward vector.

3. Free mode

An oscillatory unstable mode emerges from the time integration of the model, whose latitude–time structure is shown in Fig. 2a. It oscillates with a period of 11.5 yr and grows with an *e*-folding time of 2 yr. In this section all the growth rates cited are for zero Newtonian cooling ($b = 0$). It is clear from (2.8) that a nonzero b does nothing other than reducing the growth rate. Within 20° of the equator, the modal structure is characterized by a standing dipole that oscillates like a seesaw astride the equator. The centers of action are located at 15°. Cross-equatorial winds also oscillate with this SST seesaw, blowing from the cold into the warm hemisphere. These spatial characteristics are reminiscent of the dipole pattern in observations and the one simulated by the semiempirical model (Chang et al. 1997). Since the present model explicitly computes both surface heat flux and wind velocity, we can trace the whole feedback loop that causes the instability.

Figure 3 shows the meridional structures of the unstable mode at $t = 8.5$ yr. Within 15° of the equator, the zonal wind and SST variabilities are positively correlated, with anomalous westerly (easterly) wind appearing over a positive (negative) SST anomaly. This positive feedback between zonal wind and SST through surface latent heat flux is the mechanism that causes the amplitude of the dipole mode to grow with time. Poleward of the dipole centers, on the other hand, zonal wind and SST are roughly 90° out of phase, with *U* reaching a maximum at *T*'s nodal points. Consider a positive SST anomaly in the Northern Hemisphere. A low pressure center forms over the SST anomaly, inducing westerly (easterly) wind anomalies south (north) of the SST anomaly. In background easterly winds, these wind anomalies induce latent heat flux anomalies that act to increase (reduce) SST south (north) of the initial SST anomaly. Thus, the WES feedback off the equator causes the coupled disturbance to propagate equatorward. Equatorward propagating signals are weak but

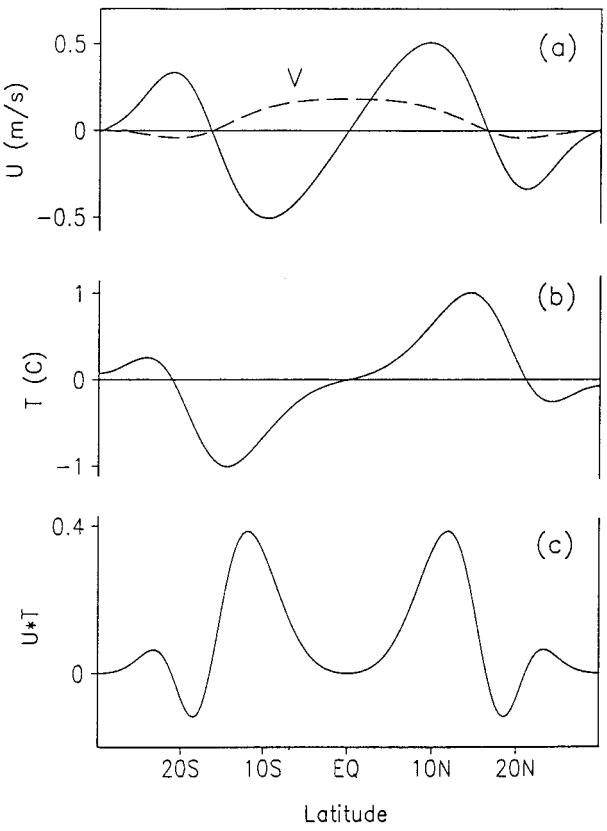

FIG. 3. Meridional structures of the decadal dipole oscillation at $t = 8.5$ yr: (a) meridional (dashed) and zonal (solid) wind components, (b) SST, and (c) the destabilization term UT.

visible poleward of 15° (Fig. 3a), eroding the dipole and eventually causing it to switch sign.

The mean state has an important effect on the time-spatial structures of the dipole mode. Figure 2b shows a case where the advection term by the mean poleward Ekman flow is removed from (2.4). The equatorward propagation becomes much more pronounced and the period of the oscillation shortens to 5 yr. It is hard to define a center of action in this case but the maximum amplitude is reached between 5° and 10° latitude. The growth rate slightly decreases due to changes in modal structures. This equatorward propagating WES mode is previously discussed by Xie (1997). The poleward Ekman flow induced by climatological easterly wind slows this equatorward propagation and hence reduces the frequency of the oscillation. The effect of this Ekman advection varies in space. Fastest just off the equator, the mean Ekman flow stops the equatorward propagation all together and establishes a quasi-stationary dipole. The Ekman flow weakens at higher latitudes, allowing a slow equatorward propagation. A similar oscillation mechanism is noted independently by Carton (1997). Chang et al. (1997) propose an alternative mechanism involving advection by the ocean gyre circulation, a difference that may be attributable to their model for-

Unauthenticated | Downloaded 05/27/24 07:30 AM UTC

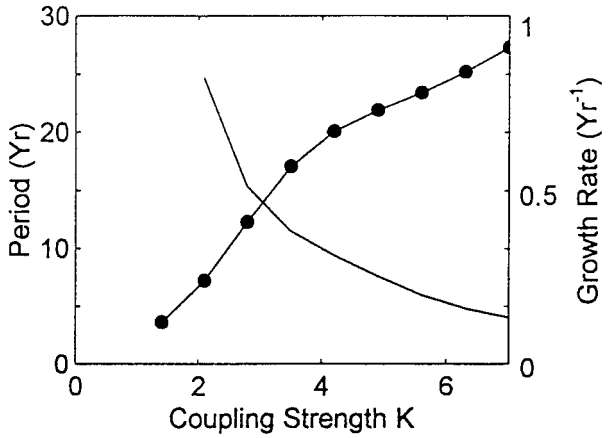

FIG. 4. Period (solid line) and growth rate (dots) of the dipole oscillation as functions of coupling coefficient (K in 10^{-2} m s^{-1} K^{-1}).

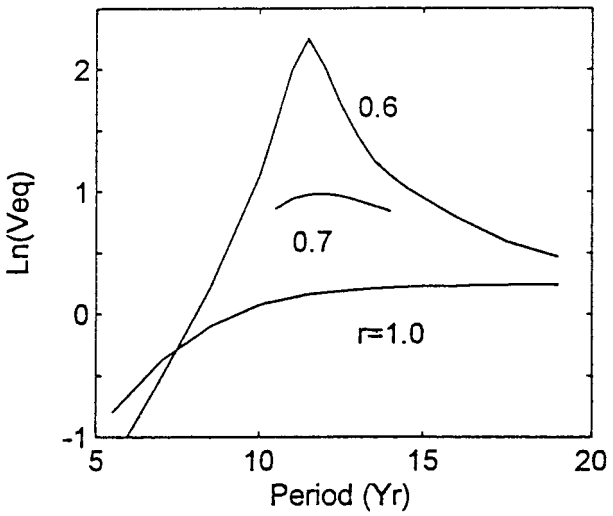

FIG. 5. Logarithm of forced cross-equatorial wind speed as a function of forcing period.

mulation. The spatial structure of surface heat flux is empirically prescribed in their model whereas it is internally determined in the present model.

Figure 4 displays the period and the growth rate of the unstable mode as functions of coupling coefficient K. At low coupling, the dominant mode is stationary. As K increases, the mode grows faster and starts to oscillate. The equatorward propagation accelerates with increasing K, causing a decrease in oscillation period. This dependence on coupling strength is similar to that in Chang et al.'s (1997) model.

4. Forced mode

The rate of thermal damping due to the temperature dependence of evaporation can be estimated from (2.5)

$$b_0 = \left(\frac{L}{R^*\overline{T}^2}\right)\frac{\overline{E}}{c_p\rho h} = (\text{yr})^{-1}, \tag{4.1}$$

for a basic state with 4 m s^{-1} wind speed and 30°C temperature. This damping rate is twice as large as the growth rate of the decadal dipole mode so the oscillation described above cannot be self-sustained. Being the least damped, the dipole mode may still stand out under weather noise or other external forcing. This section investigates the model response to periodic forcing that is applied to (2.4) as a perturbation to the equilibrium temperature of the Newtonian cooling so the governing equation for SST becomes

$$T_t + \overline{v}T_y + v\overline{T}_y = aU - b(T - \tilde{T}) + \kappa T_{yy}. \tag{4.2}$$

Note that the external forcing can also be interpreted as that associated with wind variability, $\tilde{U} = b\tilde{T}/a$. We let the imposed temperature perturbation

$$\tilde{T} = Fy\sin(\omega t) \tag{4.3}$$

have a constant amplitude at all frequencies (white noise spectrum). By varying the angular frequency ω, we can obtain a frequency–amplitude spectrum of the model response. Equatorially asymmetric weather noises are abundant in the Atlantic, with examples including the easterly waves along the northern ITCZ and vacillations of the midlatitude westerly jets. The model response is not sensitive to the meridional structure of forcing so here we choose a linear function of latitude. Forcing amplitude does not affect the shape of the spectrum in this linear model and is arbitrarily set at $F = 1$°C (3000 km)$^{-1}$ corresponding to an amplitude of 1°C at the poleward boundaries.

Figure 5 displays the amplitude of meridional wind speed at the equator as a function of forcing period. When the thermal damping is weak ($r \equiv b/b_0 = 0.6$), a sharp peak appears at the free mode's intrinsic period (11.5 yr) as a result of resonance. As the damping rate increases, the spectrum peak becomes less pronounced and shifts toward longer periods (12 yr for $r = 0.7$ and 12.5 yr for $r = 0.8$). At a high damping rate ($r = 1$), the amplitude spectrum is red without a peak at finite periods. This spectrum dependence on the damping rate is similar to that of a damped linear pendulum. As $r = 1$ is a lower limit for the realistic damping rate, the real Atlantic falls into the high damping regime that features a red spectrum. This may leave an impression that the WES feedback is not important under realistic damping. The spatial structures of the model response (Fig. 6) indicates otherwise, however. A pronounced dipole pattern dominates the SST field, a structure that bears little resemblance to the forcing function (4.3) and is a manifestation of the WES feedback.

Observed interhemispherically coherent dipole variability seems to show preferred time scales from 10 to 20 yr (Mehta and Delworth 1995). Under realistic thermal damping, such a spectral peak is not possible in the model unless the forcing has a peak at the same periods. One possibility is that such a decadal forcing comes from the extratropics. In fact, significant decadal vari-

Unauthenticated | Downloaded 05/27/24 07:30 AM UTC

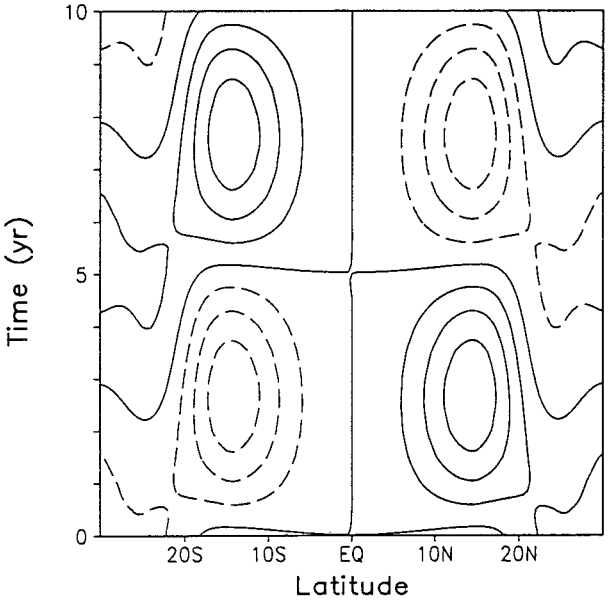

FIG. 6. Latitude–time section of sea surface temperature response to a forcing of 10-yr period confined to poleward of 25°. Note its similarity to the free mode in Fig. 2a.

ability is observed in both the North (Deser and Blackmon 1993) and South (Venegas et al. 1996) Atlantic. To explore this possibility, we conduct an experiment where the external forcing is confined to small regions poleward of 25°. A dipole pattern dominates the SST anomaly field (Fig. 6), occupying a tropical region that is free of external forcing. The WES feedback may not give rise to a preferred timescale but is clearly at work to maintain such a coherent dipole structure. Such a dipole response is seen at all forcing periods that are longer than a few years.

5. Discussion

A dipole SST mode that resembles the observed decadal variability over the tropical Atlantic is shown to exist in a dynamic ocean–atmosphere model, confirming the results from a semi-empirical model (Chang et al. 1997). In the model SST anomalies are caused by surface heat flux and advected by surface Ekman flow. Consistent with ocean GCM (Carton et al. 1996) and observational (Wagner 1996) studies, a wind–evaporation SST feedback is responsible for the temporal growth and oscillation of the dipole mode. The advection by the mean poleward Ekman flow is important for the spatially quasi-stationary dipole structure and the long oscillation period.

Ocean memories such as those associated with the thermocline ventilation (Gu and Philander 1997; K. Hanawa 1996, personal communication) and baroclinic Rossby waves are often invoked to explain the slow timescales of decadal variability. As a complementary mechanism, ocean–atmosphere coupling itself can also give rise to low-frequency oscillations. In this model, neither the ocean nor the atmosphere has an intrinsic timescale, yet the phase difference between the zonal wind and SST produces a slow decadal oscillation upon coupling. For this reason the period of the free dipole mode is sensitive to the coupling strength, and an oscillatory mode is possible only when the coupling coefficient exceeds a certain threshold value.

It is unlikely, however, that the timescale of the real Atlantic variability is determined by the free WES mode as its growth rate is not large enough to overcome the thermal damping associated with surface evaporation. Under realistic damping the amplitude spectrum of the model response to a white-noise stochastic forcing is red without a peak at finite periods. If the observed tropical Atlantic dipole prefers decadal timescales as it seems to, this result suggests that such preferred time scales be determined not within the Tropics but by interaction with the midlatitudes. In support of this proposition, the observed SST and wind anomalies associated with the North Atlantic decadal variability are organized into zonal bands of alternating signs, stacked in the meridional direction and extending into the Tropics (Deser and Blackmon 1993; Kushnir 1994; Wallace et al. 1990). These extratropical anomalies could provide the forcing for the Tropics, under which the WES feedback acts to produce a coherent interhemispheric seesaw (Xie and Tanimoto 1998). The tropical SST dipole could further feedback onto the extratropical variability via atmospheric teleconnections. The cause of the North Atlantic decadal variability is not yet clear, but candidates include the instability of ocean thermohaline circulation (Weaver and Sarachik 1991) and Arctic sea ice outflow as seen in the Great Salinity Anomaly (Dickson et al. 1988). As in the Tropics, wind-induced changes in evaporation and Ekman advection remain an important mechanism for extratropical SST variability (Alexender 1990; Cayan 1992). How the tropical and midlatitude modes of decadal variability interact in the Atlantic and how they attain the preferred decadal timescales need further investigation.

Here we have restricted our discussion to a zonally symmetric case that seems relevant to the tropical Atlantic dipole. However, the zonal extent of the oceans is an important parameter for the development of other coupled instabilities: Equatorial modes are unstable in the larger Pacific but are weakly damped in the Atlantic (Yamagata 1985; Battisti and Hirst 1989). This may explain why ENSO dominates the Pacific whereas both interannual equatorial and decadal dipole modes are observed in the Atlantic. We are currently investigating this matter.

Acknowledgments. I would like to thank T. Matsuno, P. Chang, A. Kubokawa, and L. Mysak for helpful discussions and the late T. Nitta for useful comments. This work is supported by grants from the Ministry of Education and CCSR/University of Tokyo.

Unauthenticated | Downloaded 05/27/24 07:30 AM UTC

REFERENCES

Alexander, M. A., 1990: Simulation of the response of the North Pacific Ocean to the anomalous atmospheric circulation associated with El Nino. *Climate Dyn.,* **5,** 53–65.

Battisti, D. S., and A. C. Hirst, 1989: Interannual variability in a tropical atmosphere–ocean model: Influence of the basic state, ocean geometry, and nonlinearity. *J. Atmos. Sci.,* **46,** 1687–1712.

Carton, J. A., 1997: Sea-saw sea. *Nature,* **385,** 487–488.

——, X. Cao, B. S. Giese, and A. M. da Silva, 1996: Decadal and interannual SST variability in the tropical Atlantic Ocean. *J. Phys. Oceanogr.,* **26,** 1165–1175.

Cayan, D. R., 1992: Latent and sensible heat flux anomalies over the northern oceans: Driving the sea surface temperature. *J. Phys. Oceanogr.,* **22,** 859–881.

Chang, P., L. Ji, and H. Li, 1997: A decadal climate variation in the tropical Atlantic ocean from thermodynamic air–sea interactions. *Nature,* **385,** 516–518.

Deser, C., and M. L. Blackmon, 1993: Surface climate variations over the North Atlantic Ocean during winter. *J. Climate,* **6,** 1743–1753.

Dickson, R. R., J. Meincke, S. A. Malmberg, and A. J. Lee, 1988: The ''great salinity anomaly'' in the northern North Atlantic 1968–1982. *Progress in Oceanography,* Vol. 20, Pergamon Press, 103–151.

Gill, A. E., 1980: Some simple solutions for heat-induced tropical circulation. *Quart. J. Roy. Meteor. Soc.,* **106,** 447–462.

Gu, D., and S. G. H. Philander, 1997: Interdecadal climate fluctuations that depend on exchanges between the tropics and extratropics. *Science,* **275,** 805–807.

Hasternrath, S., and L. Heller, 1977: Dynamics of climatic hazards in northeast Brazil. *Quart. J. Roy. Meteor. Soc.,* **103,** 77–92.

Kushnir, Y., 1994: Interdecadal variation in North Atlantic sea surface temperature and associated atmospheric conditions. *J. Climate,* **7,** 141–157.

Lamb, P. J., 1978: Large-scale tropical Atlantic surface circulation patterns associated with subsahara weather anomalies. *Tellus,* **30,** 240–251.

Lindzen, R. S., and S. Nigam, 1987: On the role of sea surface temperature gradients in forcing low level winds and convergence in the Tropics. *J. Atmos. Sci.,* **44,** 2418–2436.

Matsuno, T., 1966: Quasi-geostrophic motions in the equatorial area. *J. Meteor. Soc. Japan,* **44,** 25–43.

Mehta, V. M., and T. Delworth, 1995: Decadal variability of the tropical Atlantic ocean surface temperature in shipboard measurements and in a global ocean–atmosphere model. *J. Climate,* **8,** 172–190.

Moura, A. D., and J. Shukla, 1981: On the dynamics of droughts in northeast Brazil: Observations, theory, and numerical experiments with a general circulation model. *J. Atmos. Sci.,* **38,** 2653–2675.

Neelin, J. D., 1989: On the interpretation of the Gill model. *J. Atmos. Sci.,* **46,** 2466–2468.

Nobre, P., and J. Shukla, 1996: Variations of sea surface temperature, wind stress, and rainfall over the tropical Atlantic and South America. *J. Climate,* **9,** 2464–2479.

Venegas, S. A., L. A. Mysak, and D. N. Straub, 1996: Evidence for interannual and interdecadal climate variability in the South Atlantic. *Geophys. Res. Lett.,* **23,** 2673–2676.

Wagner, R. G., 1996: Mechanisms controlling variability of the interhemispheric sea surface temperature gradient in the tropical Atlantic. *J. Climate,* **9,** 2010–2019.

Wallace, J. M., C. Smith, and Q.-R. Jiang, 1990: Spatial patterns of atmosphere/ocean interaction in the northern winter. *J. Climate,* **3,** 990–998.

Weaver, A. J., and E. S. Sarachik, 1991: Evidence for decadal variability in an ocean general circulation model: An advective mechanism. *Atmos.–Ocean,* **29,** 197–231.

Woodruff, S. D., R. J. Slutz, R. L. Jenne, and P. M. Steurer, 1987: A comprehensive ocean–atmosphere dataset. *Bull. Amer. Meteor. Soc.,* **68,** 521–527.

Xie, S.-P., 1996: Westward propagation of latitudinal asymmetry in a coupled ocean–atmosphere model. *J. Atmos. Sci.,* **53,** 3236–3250.

——, 1997: Unstable transition of the tropical climate to an equatorially asymmetric state in a coupled ocean–atmosphere model. *Mon. Wea. Rev.,* **125,** 667–679.

——, and S. G. H. Philander, 1994: A coupled ocean–atmosphere model of relevance to the ITCZ in the eastern Pacific. *Tellus,* **46A,** 340–350.

——, and Y. Tanimoto, 1998: A pan-Atlantic decadal climate oscillation. *Geophys. Res. Lett.,* **25,** 2185–2188.

Yamagata, T., 1985: Stability of a simple air-sea coupled model in the Tropics. *Coupled Ocean Atmosphere Models,* J. C. J. Nihoul, Ed., Elsevier, 637–658.

Zebiak, S. E., 1993: Air–sea interaction in the equatorial Atlantic region. *J. Climate,* **6,** 1567–1586.

——, and M. A. Cane, 1987: A model El Niño–Southern Oscillation. *Mon. Wea. Rev.,* **115,** 2262–2278.

Unauthenticated | Downloaded 05/27/24 07:30 AM UTC